


# Circulating miR-203 derived from metastatic tissues promotes myopenia in colorectal cancer patients

Yoshinaga Okugawa<sup>1\*</sup> , Yuji Toiyama<sup>1\*</sup>, Keun Hur<sup>2</sup>, Akira Yamamoto<sup>1</sup>, Chengzeng Yin<sup>1</sup>, Shozo Ide<sup>1</sup>, Takahito Kitajima<sup>1</sup>, Hiroyuki Fujikawa<sup>1</sup>, Hiromi Yasuda<sup>1</sup>, Yuhki Koike<sup>1</sup>, Yoshiki Okita<sup>1</sup>, Junichiro Hiro<sup>1</sup>, Shigeyuki Yoshiyama<sup>1</sup>, Toshimitsu Araki<sup>1</sup>, Chikao Miki<sup>3</sup>, Donald C. McMillan<sup>4</sup>, Ajay Goel<sup>5</sup> & Masato Kusunoki<sup>1</sup>

<sup>1</sup>Department of Gastrointestinal and Pediatric Surgery, Division of Reparative Medicine, Institute of Life Sciences, Mie University Graduate School of Medicine, Japan, <sup>2</sup>Department of Biochemistry and Cell Biology, School of Medicine, Kyungpook National University, Daegu, Korea, <sup>3</sup>Department of Surgery, Iga Municipal Ueno General Citizen's Hospital, Iga, Mie, Japan, <sup>4</sup>Academic Unit of Surgery, School of Medicine, University of Glasgow, Glasgow Royal Infirmary, Glasgow, UK, <sup>5</sup>Center for Gastrointestinal Research, Center for Translational Genomics and Oncology, Baylor Scott & White Research Institute, Charles A. Sammons Cancer Center, Baylor University Medical Center, Dallas, TX, USA

## Abstract

**Background** Sarcopenia frequently occurs in metastatic cancer patients. Emerging evidence has revealed that various secretory products from metastatic tumours can influence host organs and promote sarcopenia in patients with malignancies. Furthermore, the biological functions of microRNAs in cell-to-cell communication by incorporating into neighbouring or distal cells, which have been gradually elucidated in various diseases, including sarcopenia, have been elucidated.

**Methods** We evaluated psoas muscle mass index (PMI) and intramuscular adipose tissue content (IMAC) using pre-operative computed tomography imaging in 183 colorectal cancer (CRC) patients. miR-203 expression levels in CRC tissues and pre-operative serum were evaluated using quantitative polymerase chain reaction. Functional analysis of miR-203 overexpression was investigated in human skeletal muscle cells (SkMCs), and cells were analysed for proliferation and apoptosis. Expressions of several putative miR-203 target genes (CASP3, CASP10, BIRC5, BMI1, BIRC2, and BIRC3) in SKMCs were validated.

**Results** A total of 183 patients (108 men and 75 women) were included. The median age of enrolled patients at diagnosis was 68.0 years (range 35–89 years). High IMAC status significantly correlated with female gender ( $P = 0.004$ ) and older age ( $P = 0.0003$ ); however, no other clinicopathological factors correlated with IMAC status in CRC patients. In contrast, decreased PMI significantly correlated with female gender ( $P = 0.006$ ) and all well-established disease development factors, including advanced T stage ( $P = 0.035$ ), presence of venous invasion ( $P = 0.034$ ), lymphovascular invasion ( $P = 0.012$ ), lymph node ( $P = 0.001$ ), distant metastasis ( $P = 0.002$ ), and advanced Union for International Cancer Control tumour–node–metastasis stage classification ( $P = 0.0004$ ). Although both high IMAC status and low PMI status significantly correlated with poor overall survival (IMAC:  $P = 0.0002$ ; PMI:  $P < 0.0001$ ; log-rank test) and disease-free survival (IMAC:  $P = 0.0003$ ; PMI:  $P = 0.0002$ ; log-rank test), multivariate Cox's regression analysis revealed that low PMI was an independent prognostic factor for both overall survival (hazard ratio: 4.69, 95% confidence interval (CI): 2.19–10,  $P = 0.0001$ ) and disease-free survival (hazard ratio: 2.33, 95% CI: 1.14–4.77,  $P = 0.021$ ) in CRC patients. Serum miR-203 expression negatively correlated with pre-operative PMI level ( $P = 0.0001$ ,  $\rho = -0.25$ ), and multivariate logistic regression analysis revealed that elevated serum miR-203 was an independent risk factor for myopenia (low PMI) in CRC patients (odds ratio: 5.16, 95% CI: 1.8–14.8,  $P = 0.002$ ). Overexpression of miR-203 inhibited cell proliferation and induced apoptosis via down-regulation of BIRC5 (survivin) expression in human SkMC line.

**Conclusions** Assessment of serum miR-203 expression could be used for risk assessment of myopenia, and miR-203 might be a novel therapeutic target for inhibition of myopenia in CRC.

**Keywords** Colorectal cancer; Myopenia; miR-203; Metastasis; Apoptosis; BIRC5

Received: 30 August 2018; Accepted: 9 January 2019

\*Correspondence to: Yoshinaga Okugawa and Yuji Toiyama, Department of Gastrointestinal and Pediatric Surgery, Division of Reparative Medicine, Institute of Life Sciences, Mie University Graduate School of Medicine, 2-174 Edobashi, Tsu, Mie 514-8507, Japan. Tel: +81-592-31-5294, Fax: +81-592-32-6968.

Email: yoshinaga.okugawa@gmail.com; ytoi0725@clin.medic.mie-u.ac.jp

<sup>†</sup>Both authors contributed equally for this study.

## Introduction

Cancer cachexia is defined as a 'multi-factorial, systemic syndrome characterized by weight loss due to loss of skeletal muscle mass (sarcopenia)'.<sup>1</sup> Several lines of evidence have suggested that alteration of muscle cell homeostasis via deterioration and decreased synthesis of muscle proteins can promote muscle cell loss in patients with malignancies.<sup>2–4</sup> Furthermore, a pattern of sarcopenia (myopenia and myosteosis) and this clinical burden as a feasible indicator of poor prognosis in cancer patients is gradually elucidated.<sup>5–8</sup>

Metastasis is the systemic dissemination of cancer cells from the primary tumour site,<sup>9</sup> and sarcopenia is commonly observed in advanced cancer patients with distant metastases.<sup>10,11</sup> A close link between metastasis and sarcopenia has been demonstrated in various types of cancers, including colorectal cancer (CRC).<sup>10,12,13</sup> Furthermore, recent studies have revealed that various secretory products, including soluble proteins, metabolites, and exosomes, from metastatic tumours can influence host organs and promote sarcopenia in patients with malignancies.<sup>10,14,15</sup> However, the detailed mechanism underlying the development of sarcopenia in metastatic cancer patients remains unclear.

MicroRNAs (miRNAs) are a class of small single-stranded RNAs approximately 18–25 nucleotides in length that are involved in various essential biological processes, such as development, cellular differentiation, proliferation, and apoptosis.<sup>16–18</sup> Exosome-encapsulated miRNAs are secreted from various tissues and can stably exist in systemic circulation. Recent studies have revealed the capability of these miRNAs to exert biological functions by incorporating into neighbouring or distal cells.<sup>19,20</sup>

A recent study from our research group demonstrated that miR-203 (official name: miR-203a-3p, gene ID: 406986) is one of the most representative secretory miRNAs in CRC patients and that circulating miR-203 originated from metastatic tissues, not primary cancerous tissues.<sup>21</sup> Furthermore, other studies demonstrated that transient expression of miR-203 inhibits cell differentiation in various types of cells, including skin cells and skeletal muscle cells (SkMCs).<sup>22,23</sup>

In this study, we systemically assessed the clinical significance of pre-operative myopenia and myosteosis in CRC patients. We further evaluated the expression of the metastasis-related miR-203 in primary tissues and matched serum specimens from these patients to evaluate the correlation between miR-203 expression and body composition (BC) alteration in CRC patients. We also performed a series of *in vitro* analyses using a human SkMC line to clarify the biological role of miR-203 in the development of sarcopenia in advanced cancer patients with metastasis.

## Material and methods

### Patients

A total of 183 patients undergoing surgery for resection of primary CRC tumours at Mie University Hospital were enrolled in this study. None of the patients received chemotherapy or radiotherapy prior to surgery, and no peri-operative mortality was observed. The median age of the patients at diagnosis was 68.0 years (range 35–89 years). The diagnosis of CRC was confirmed in all 183 patients based on clinicopathological findings. The tumour–node–metastasis staging system from the American Joint Committee on Cancer was used for the pathological tumour staging of CRC.<sup>24</sup> The locations of tumours and distant metastases were determined by barium enema, colonoscopy, computed tomography (CT), and magnetic resonance imaging. Resection of the primary tumour was performed in all patients, and all patients were followed up for tumour recurrence at regular intervals for up to 5 years. During each annual hospital visit, all patients underwent a chest X-ray, colonoscopy, and abdominal CT. Patients treated with radiotherapy or chemotherapy before surgery were excluded from this study. All patients were classified according to Union for International Cancer Control stage classification of resected specimens: 37 patients had Stage I disease, 61 had Stage II, 44 had Stage III, and 41 had Stage IV. All CRC patients with Stage III/IV disease received 5-fluorouracil-based chemotherapy, whereas no adjuvant chemotherapy was given to Stage I and II patients. Patients were observed at 3 month intervals for 24 months after completion of surgery, followed by every 6 months for 3 years and then yearly. A history was taken, and a physical examination was performed at each visit, and chest X-ray, colonoscopy, and CT were performed annually. All participants provided informed written consent, and the study protocol was approved by the Institutional Review Board of our institution.

### Image analysis

The height data of all patients were recorded, and pre-operative CT scan was assessed within 4 weeks before surgery. Pre-operative CT scan images were stored in an electronic format suitable for image analysis to assess the BC status. Using pre-operative plain CT at superior aspect of the fourth lumbar vertebra as previously described,<sup>13,25,26</sup> we measured the cross-sectional area of the bilateral psoas muscles by manual tracing, and then the psoas muscle mass index (PMI) was calculated as follows: PMI = cross-sectional area of bilateral psoas muscle height<sup>2</sup> (cm<sup>2</sup>/m<sup>2</sup>). Low PMI was regarded as a proxy for low muscle volume, as previously described.<sup>6–8</sup> Subfascial muscular tissue in the multifidus muscle was estimated by manual tracing at the same level

on pre-operative plain CT images, and mean CT values [Hounsfield unit (HU)] for these areas were determined with the Aquarius NET server (Tera Recon, Inc., San Mateo, CA, USA). We placed four circles on areas of subcutaneous fat away from major vessels in CT images that were used as the region of interest (ROI) of subcutaneous fat. The mean CT values (HU) for the ROI of subcutaneous fat were also measured. Intramuscular adipose tissue content (IMAC) was calculated by the ratio of these CT values, as previously reported by Kitajima *et al.*,<sup>27,28</sup> as follows: IMAC = mean CT value of ROI of multifidus muscle (HU) / mean CT value of ROI of subcutaneous fat (HU). High IMAC was regarded as a proxy for low muscle quality.

### Sample collection

We obtained surgical tissue specimens and matched pre-operative serum specimens from CRC patients in this study. All of these patients were previously described as a validation cohort in a biomarker study of serum miR-203.<sup>21</sup> Blood samples were obtained by venipuncture before surgery. Each sample was centrifuged at  $3000 \times g$  for 5 min and stored at  $-80^\circ\text{C}$  until analysis.

### RNA isolation and quantitative reverse transcription polymerase chain reaction from serum samples

RNA extraction and miRNA enrichment from all serum samples were performed using the Qiagen miRNeasy Kit (Qiagen, Valencia, CA, USA) according to the manufacturer's instructions. Briefly, 200  $\mu\text{L}$  of serum was thawed on ice and centrifuged at  $3000 \times g$  for 5 min to remove cell debris. Next, 200  $\mu\text{L}$  of the supernatant was lysed in 5 volumes of Qiazol solution. To normalize any inadvertent sample-to-sample variations during the RNA isolation procedure, reverse transcription (RT), and PCR, 25 fmol of synthetic *Caenorhabditis elegans* miRNA (cel-miR-39) was added to each denatured sample. Small RNAs were then enriched and purified following the manufacturer's protocol, with the exception that the enriched small RNAs were eluted in 40  $\mu\text{L}$  of nuclease-free water. For miRNA-based RT-PCR assays, 1.67  $\mu\text{L}$  of enriched small RNAs from serum or cell culture medium were reverse transcribed using the TaqMan MicroRNA Reverse Transcription Kit (Applied Biosystems, Foster City, CA, USA) in a total volume of 5  $\mu\text{L}$ , according to the manufacturer's instructions. A 1:15 dilution of the RT products was used as template for the PCR. PCRs for quantifying miR-203 and cel-miR-39 were performed in duplicate, with TaqMan 2 $\times$  Universal PCR Master Mix, using conditions previously described.<sup>29,30</sup>

### RNA isolation and quantitative reverse transcription polymerase chain reaction from formalin-fixed, paraffin-embedded tissues

Total RNA was isolated from formalin-fixed, paraffin-embedded samples using the RecoverAll Total Nucleic Acid Isolation Kit (Ambion Inc., Austin, TX, USA) according to the manufacturer's instructions. Briefly, tissue sections were microdissected to enrich for neoplastic cells, followed by deparaffinization and RNA extraction using the manufacturer's protocol. Total RNA was eluted in the appropriate buffer and quantified using a NanoDrop Spectrophotometer (NanoDrop Technologies, Wilmington, DE, USA). RT reactions were carried out using the TaqMan MicroRNA Reverse Transcription Kit (Applied Biosystems, Foster City, CA, USA) in a total reaction volume of 15  $\mu\text{L}$ . MiR-16 was chosen as the endogenous normalizer for miRNAs based on previous findings that miR-16 is one of the most suitable reference genes for relative quantification of small non-coding RNAs in colonic tissues including with CRC and normal colonic mucosa from microarray analysis of large cohorts; in addition, we previously demonstrated that miR-16 is a reliable normalizer for tissue samples.<sup>21,30–35</sup> MiR-203 and miR-16 were quantified by quantitative reverse transcription polymerase chain reaction (qRT-PCR) using MicroRNA Assay Kits (Applied Biosystems) in duplicate reactions. qRT-PCR was performed on an Applied Biosystems 7000 Sequence Detection System with the following cycling conditions:  $95^\circ\text{C}$  for 10 min, followed by 45 cycles of  $95^\circ\text{C}$  for 15 s and  $60^\circ\text{C}$  for 1 min. Cycle threshold (Ct) values were calculated using the same threshold cut-off values for each assay to prevent plate-to-plate variations. Data were analysed using the sds 1.4 software (Applied Biosystems, Foster City, CA, USA). PCRs for quantifying miR-203 and miR-16 were performed in duplicate reactions with TaqMan 2 $\times$  Universal PCR Master Mix.

### Calculation of microRNA expression

Expression levels of miRNAs were normalized using cel-miR-39 (for serum samples) and miR-16 (for tissue samples) using the  $2^{-\Delta\text{Ct}}$  method, as previously described.<sup>21,30–32,34,35</sup> Differences between the groups are presented as  $\Delta\text{Ct}$ , indicating differences between Ct values of miRNAs of interest and Ct values of normalizer miRNAs.

### Cell line

The human SkMC line was purchased from Promo Cell (Heidelberg, Germany) and maintained in Skeletal Muscle Cell Growth Medium (Promo Cell) at  $37^\circ\text{C}$  in 5% humidified  $\text{CO}_2$  atmosphere.

### Transfection of miR-203 mimic molecules

To induce miR-203 expression, cells were transfected with *mirVana* hsa-miR-203-3p mimic (miR-203 mimic, Applied Biosystems) using Lipofectamine 2000 (Invitrogen). A *mirVana* miRNA mimic negative control (Applied Biosystems) containing a random sequence with no identifiable effects on functions of known miRNAs was used as a negative control. The final oligonucleotide concentration was 50 nM. Cells were transfected for 48 h before analysis.

### Cell proliferation assay

Cell proliferation was evaluated with a WST-8 colorimetric assay kit (Cell Counting Kit-8, Dojindo Laboratories, Tokyo, Japan). Forty-eight hours after transfection of SkMCs with miR-203 mimic or negative control mimic, cells were seeded at  $5 \times 10^3$  cells per well in 96-well flat-bottomed microtitre plates in a final volume of 100  $\mu$ L culture medium per well and incubated in a humidified atmosphere. After 0–7 days of culture, 10  $\mu$ L Cell Counting Kit-8 reagent was added to each well, and the plates were incubated for 1 h in a humidified atmosphere. The absorbance of each well was measured at a wavelength of 450 nm using SoftMax Pro (Molecular Devices Corp., Sunnyvale, CA, USA). Each independent experiment was performed three times.

### Cell cycle analysis and apoptosis assay

For cell cycle analysis, the DNA content of miR-203 mimic-transfected or negative control mimic-transfected SkMCs was evaluated using the Muse<sup>TM</sup> cell cycle assay kit (Millipore, Billerica, MA, USA), according to the manufacturer's instructions, on the Muse Cell Analyzer (Millipore). Each independent experiment was performed three times. The rate of apoptosis was measured in transfected cells using the annexin V and Dead Cell Assay Kit (Millipore) and the WST-8 colorimetric assay (Cell Counting Kit-8, Dojindo Laboratories) following the manufacturers' instructions.

### Total RNA extraction, complementary DNA synthesis, and quantitative reverse transcription polymerase chain reaction

Total RNA was isolated using the miRNeasy Mini Kit (Qiagen) according to the manufacturer's instructions. Complementary DNA was synthesized from 5  $\mu$ g total RNA with random hexamer primers and SuperScript III Reverse Transcriptase (Invitrogen, Carlsbad, CA, USA). qRT-PCR analysis was performed using the StepOne Real-Time PCR System (Applied

Biosystems), as previously described.<sup>36,37</sup> CASP3, CASP10, BIRC5, BMI1, BIRC2, BIRC3, and GAPDH mRNA expression levels were measured using Power SYBR Green Master Mix (Life Technologies, Carlsbad, CA, USA). Primers for CASP3, CASP10, BIRC5, BMI1, BIRC2, BIRC3, and GAPDH mRNAs were designed using PRIMER3 software (Biology Workbench Version 3.2; San Diego Supercomputer Center, University of California, San Diego, CA, USA). Sequence information of these primers is described in Table S1.

### Immunofluorescence

Primary antibody for BIRC5 (1:50, Santa Cruz, Dallas, TX, USA) was incubated overnight at 4 °C. After washing the sections five times for 5 min, Alexa Fluor 546 goat anti-mouse IgG (1:100, Invitrogen, Renfrew, UK) was used as the secondary antibody, and was incubated for 1 h at room temperature. Nuclear staining was performed with 4,6-diamidino-2-phenylindole dihydrochloride (DAPI) (ProLong Gold Antifade Reagent with DAPI; Invitrogen). Confocal images were acquired by IX71 inverted microscopy with a DP70 digital camera system (Olympus, Center Valley, PA, USA), as previously described.<sup>37</sup>

### Statistical methods

Statistical analysis was performed using MEDCALC version 16.8.4 (MedCalc Software, Ostend, Belgium). Results are expressed as medians  $\pm$  interquartile ranges. Differences between groups were estimated by the  $\chi^2$  test, one-way analysis of variance, and Mann–Whitney *U* test when appropriate. Shapiro–Wilk tests were performed to evaluate the normality of distribution, and Levene's tests were conducted to assess the equality of variance for comparable groups. Correlations between BC status and tissue or serum miR-203 expression were assessed using Spearman's rank correlation test. For time-to-event analyses, survival estimates were calculated using Kaplan–Meier analysis, and groups were compared with the log-rank test. Receiver operating characteristic (ROC) curves with Youden's index were established to determine the cut-off values for analysing prognosis in each gender. Overall survival (OS) was measured from the date the patient underwent surgery until the date of death resulting from any cause (i.e. cancer-unrelated deaths were not censored) or last known follow-up for patients that were still alive. Disease-free survival (DFS) analysis was measured from the date the patient underwent curative surgery to the date of disease recurrence, death from any cause (i.e. cancer-unrelated deaths were not censored), or until last contact with the patient. Cox's proportional hazard models were used to estimate hazard ratios (HRs) for death and recurrence. Assumptions of proportionality were confirmed for the Cox proportional hazards analyses by generating Kaplan–Meier survival curves

(e.g. high vs. low PMI groups) and by ensuring that the two curves did not intersect each other. Multivariate logistic regression models were used to predict factors influencing myopenia (low PMI). Variables with  $P < 0.05$  in the univariate analysis were included in the multivariate analysis. Clinical variables that were considered for univariate and multivariate analyses, in addition to target BC status, were previously identified confounding factors that affected the prognosis of patients with CRC: sex, age at diagnosis, pathological differentiation (differentiated or undifferentiated), T stage (T1/2 or T3/4), venous invasion (present or absent), lymphatic vessel invasion (present or absent), lymph node metastasis (present or absent), and distant metastasis (present or absent). Furthermore, we included representative nutrition markers, including haemoglobin (high or low), number of lymphocytes (high or low), and albumin (high or low) in multivariate logistic regression analysis to identify independent risk factor for myopenia in CRC patients. Cut-off thresholds for each covariate were determined by ROC analysis with Youden's index for myopenia in each gender of CRC patients. All  $P$  values were two sided, and those less than 0.05 were considered statistically significant.

## Results

### *Differences of body composition status according to sex*

Based on previous findings about the gender-related differences of BC status in CRC patients, we first assessed the relationships between sex and pre-operative BC status in CRC patients (Table S2).<sup>6–8,13</sup> In consistent with the previous reports, both PMI and IMAC showed significant differences between male and female CRC patients (PMI:  $291.3 \pm 130.6$  and  $215.9 \pm 70.7$ , respectively,  $P < 0.00001$ ; IMAC:  $-0.35 \pm 0.2$  and  $-0.24 \pm 0.22$ , respectively,  $P = 0.00002$ ). We thus set the cut-off values for PMI and IMAC using sex-specific cut-off values established by ROC curve analysis with Youden's index for survival in this cohort (male, PMI: 240.8, IMAC:  $-0.26$ ; female, PMI: 215.9, IMAC:  $-0.21$ ).

### *Low pre-operative psoas muscle mass index is significantly correlated with clinicopathological factors associated with disease progression in colorectal cancer patients*

We next evaluated the association between pre-operative BC status and clinicopathological factors in CRC patients (Table 1). High IMAC status significantly correlated with older age and female gender; however, no other oncological clinicopathological factors were correlated with IMAC status in

CRC patients. In contrast, low PMI status significantly correlated with all well-established disease development factors, including advanced T classification ( $P = 0.035$ ), presence of vessel ( $P = 0.034$ ), lymphovascular invasion ( $P = 0.012$ ), lymph node ( $P = 0.001$ ), distant metastasis ( $P = 0.002$ ), and advanced Union for International Cancer Control tumour–node–metastasis stage classification ( $P = 0.0004$ ) in CRC patients.

### *Decreased psoas muscle mass index in pre-operative status is an independent prognostic factor for both overall survival and disease-free survival in colorectal cancer patients*

We next conducted time-to-event analysis to clarify the prognostic impact of pre-operative PMI and IMAC status in CRC patients. We generated Kaplan–Meier survival curves according to PMI and IMAC status. Interestingly, both high IMAC and low PMI status significantly correlated with poor prognosis for OS and DFS in CRC patients (IMAC:  $P = 0.0002$  and  $P = 0.0003$ , respectively, Figure 1A and 1B; PMI:  $P < 0.0001$  and  $P = 0.0002$ , respectively, Figure 1C and 1D; log-rank test). Furthermore, the prognostic impacts of pre-operative PMI and IMAC were consistent in both male gender and female gender in this cohort (Figure S1A–S1H).

To determine the potential of pre-operative BC status as a predictive biomarker of recurrence and prognosis in CRC patients, we next performed multivariate Cox's regression analysis. In addition to lymph node metastasis and distant metastasis, low pre-operative PMI was also an independent prognostic factor for OS in CRC patients (HR: 4.69, 95% confidence interval (CI): 2.19–10,  $P = 0.0001$ , Table 2A). Furthermore, in addition to lymph node metastasis, low pre-operative PMI was also an independent prognostic factor for poor DFS in these patients (HR: 2.33, 95% CI: 1.14–4.77,  $P = 0.021$ , Table 2B).

### *Dysregulated miR-203 expression in tissue and serum of colorectal cancer patients*

We recently revealed that circulating miR-203 originated from metastatic tissues, not primary cancerous tissues.<sup>21</sup> Combined these evidences with functional role of miR-203 in cell differentiation of SkMCs,<sup>22,23</sup> we thus next evaluated tissue and matched pre-operative serum miR-203 expression to clarify the association between miR-203 expression levels and pre-operative BC status in CRC patients. Pre-operative IMAC status was not associated with tissue or serum miR-203 expression in CRC patients (Figure 1E). In contrast, the association between PMI status and miR-203 expression demonstrated engaging findings. miR-203 expression in primary cancerous tissues was significantly decreased in low PMI patients compared with those in high PMI patients ( $P = 0.03$ , Figure 1F). On the other hand, pre-operative serum miR-203

**Table 1** Correlation between clinicopathological variables and PMI and IMAC in colorectal cancer patients

Variable	n	PMI		P value	IMAC		P value
		High (n = 112)	Low (n = 71)		High (n = 52)	Low (n = 131)	
Gender							
Male	108	75	33	<b>0.006*</b>	22	86	<b>0.004*</b>
Female	75	37	38		30	45	
Age (years)							
≥68 <sup>a</sup>	95	63	32	0.14	16	79	<b>0.0003*</b>
>68	88	49	39		36	52	
Histological type							
Differentiated	167	105	62	0.13	47	120	0.79
Undifferentiated	16	7	9		5	11	
Location							
Right	58	31	27	0.14	20	38	0.22
Left	125	81	44		32	93	
Pathological T category							
pT1/2	58	42	16	<b>0.035*</b>	13	45	0.22
pT3/4	125	70	55		39	86	
Vessel invasion							
Present	75	39	36	<b>0.034*</b>	27	48	0.06
Absent	108	73	35		25	83	
Lymphovascular invasion							
Present	136	76	60	<b>0.012*</b>	43	93	0.1
Absent	47	36	11		9	38	
Lymph node metastasis							
Present	76	36	40	<b>0.001*</b>	26	50	0.14
Absent	107	76	31		26	81	
Distant metastasis							
Present	40	16	24	<b>0.002*</b>	14	26	0.3
Absent	143	96	47		38	105	
UICC TNM classification							
Stage I	37	29	8	<b>0.0004*</b>	9	28	0.17
Stage II	61	41	20		14	47	
Stage III	44	25	19		15	29	
Stage IV	41	17	24		14	27	

IMAC, intramuscular adipose tissue content; PMI, psoas muscle mass index; TNM, tumour–node–metastasis; UICC, Union for International Cancer Control.

<sup>a</sup>The median age at surgery in this cohort was 68 years.

\* $P < 0.05$ . Bold font means significant  $p$ -value in these tables.

expression showed an opposite trend and was significantly increased in low PMI patients compared with high PMI patients ( $P = 0.014$ , Figure 1F). Furthermore, to elucidate the direct correlation in each of these levels, we used Spearman's rank correlation test and found that IMAC levels were not correlated with tissue or serum miR-203 expression in CRC patients (Figure 1G). Surprisingly, despite the lack of significant correlation between PMI status and miR-203 expression in cancer tissues, serum miR-203 expression was negatively correlated with pre-operative PMI in CRC patients ( $P = 0.001$ ,  $\rho = -0.25$ , Figure 1H).

### *Elevated miR-203 level in pre-operative serum was an independent risk factor for myopenia in colorectal cancer patients*

During the last decade, various blood-based markers, such as haemoglobin, lymphocytes, and albumin, have been shown as potential analytes for the assessment of nutrition status and myopenia in patients with various malignancies.<sup>38,39</sup> In line with previously published evidence, our cohort also demonstrated

that both pre-operative haemoglobin and albumin levels were significantly decreased in CRC patients with low vs. high PMI (Figure S2A–S2C). To determine the potential of serum miR-203 as a predictive biomarker for myopenia, we next performed multivariate logistic analysis including these representative blood-based markers in CRC patients. Notably, in addition to decreased haemoglobin and albumin, elevated serum miR-203 levels emerged as one of the independent predictive factors for myopenia (odds ratio: 5.16, 95% CI: 1.8–14.8,  $P = 0.002$ , Table 3) in these patients. Collectively, these results suggest that serum miR-203 expression may serve as a clinically feasible biomarker for predicting cancer myopenia in CRC patients. Therefore, we decided to perform further assessment of the potential biological function of miR-203 in myopenia.

### *Overexpression of miR-203 inhibits cell proliferation and promotes apoptosis in human skeletal muscle cells*

As described earlier, we found that elevated expression of circulating miR-203 was negatively correlated with decreased

**Figure 1** Prognostic impact of body composition (BC) status and its correlation with tissue or serum miR-203 expression in colorectal cancer (CRC) patients (A–D). Prognostic impact of psoas muscle mass index (PMI) and intramuscular adipose tissue content (IMAC) in CRC patients. Kaplan–Meier survival curves for overall survival (OS) (A, C) and disease-free survival (DFS) (B, D) in CRC patients based on IMAC or PMI status in CRC patients. High IMAC status was significantly correlated with poor prognosis in OS ( $P = 0.0002$ ; log-rank test, A) and DFS ( $P = 0.0003$ ; log-rank test, B). Decreased PMI significantly correlated with poor prognosis for OS ( $P < 0.0001$ ; log-rank test, C) and DFS ( $P = 0.0002$ ; log-rank test, D). (E, F) MiR-203 expression in primary CRC tissues and pre-operative serum specimens according to BC status. (E, F) Association between tissue and serum miR-203 expression and BC status in CRC. (E) MiR-203 expression in primary CRC tissues (left,  $P = 0.73$ ) and pre-operative serum specimens (right,  $P = 0.83$ ) was not significantly associated with IMAC status in CRC patients. (F) Decreased miR-203 expression in primary CRC tissues (left,  $P = 0.03$ ) and elevated miR-203 expression in pre-operative serum (right,  $P = 0.014$ ) were significantly associated with low PMI status in CRC patients. Statistically significant differences were determined using the Mann–Whitney  $U$  test. Cut-off thresholds of PMI/IMAC were determined by receiver operating characteristic analysis with Youden’s index for prognosis. (G, H) Direct correlation between tissue or serum miR-203 expression and BC level in CRC patients. (G) MiR-203 expression in primary CRC tissues (left,  $P = 0.3$ ) and pre-operative serum specimens (right,  $P = 0.73$ ) did not significantly correlate with IMAC status in CRC patients. (H) No significant correlation was found between PMI level and miR-203 expression in CRC tissues (left), but serum miR-203 expression was negatively correlated with PMI level in CRC patients (right,  $P = 0.001$ ,  $\rho = -0.25$ ). Statistically significant differences were determined using the Spearman’s rank correlation test, and all statistical tests were two sided.

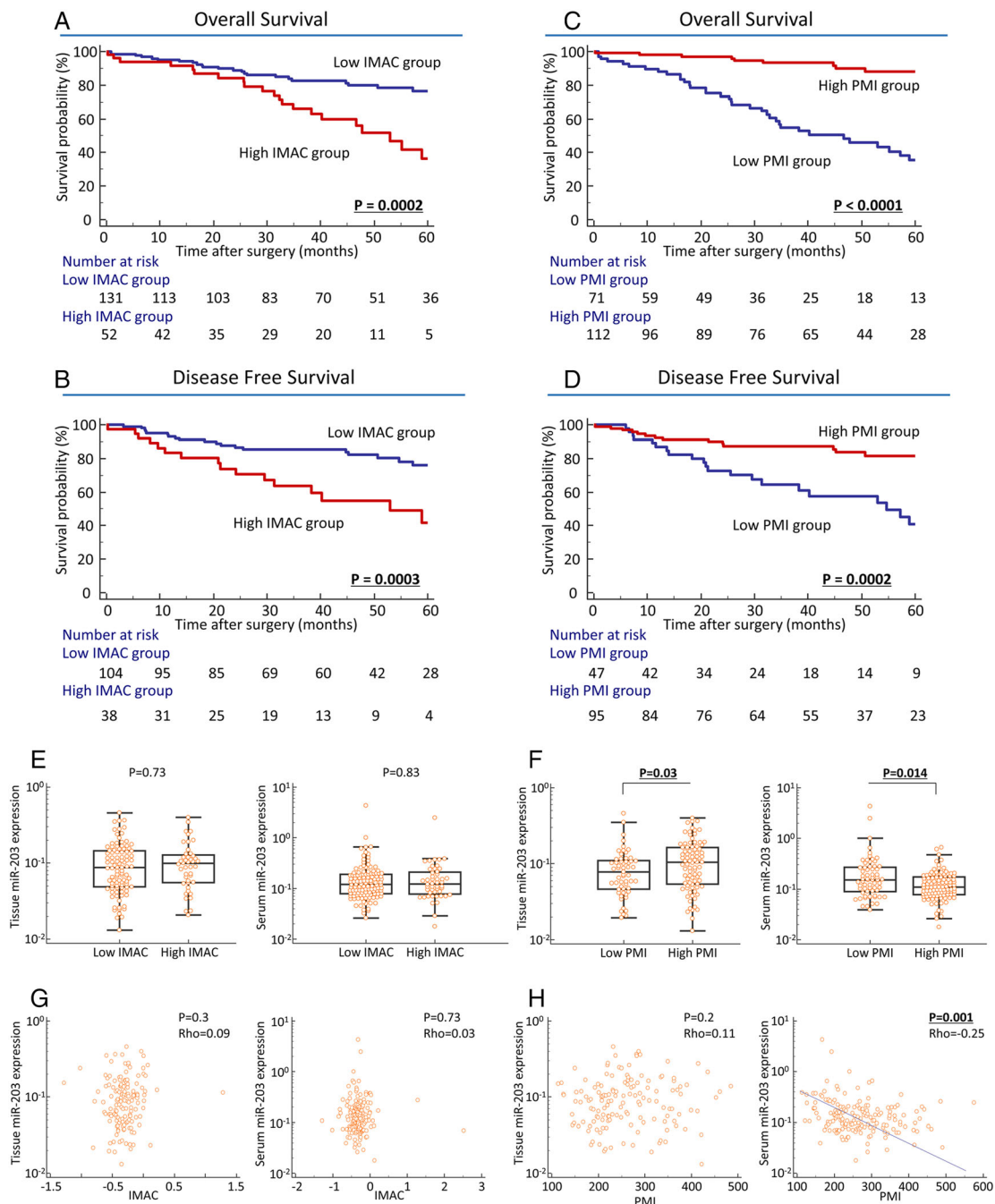


**Table 2A** Multivariate analysis for predictors of overall survival

Variable	Univariate			Multivariate		
	HR	95% CI	P value	HR	95% CI	P value
Gender (male)	0.7	0.39–1.23	0.21			
Age (>68 years old) <sup>a</sup>	1.43	0.81–2.53	0.21			
Histological type (undifferentiated)	3.1	1.45–6.63	<b>0.004*</b>	2.16	0.94–4.95	0.07
Location (left)	0.68	0.38–1.22	0.2			
T classification (pT3/4)	4.8	1.9–12.1	<b>0.0009*</b>	2.6	0.91–7.39	0.07
Vessel involvement (present)	2.42	1.35–4.33	<b>0.003*</b>	0.67	0.32–1.43	0.3
Lymphatic vessel involvement (present)	3.24	1.28–8.19	<b>0.013*</b>	1.08	0.36–3.22	0.89
Lymph node metastasis (present)	4.49	2.43–8.31	<b>&lt;0.0001*</b>	2.42	1.16–5.06	<b>0.019*</b>
Distant metastasis (present)	5.45	3.03–9.79	<b>&lt;0.0001*</b>	3.02	1.51–6.02	<b>0.002*</b>
PMI (low) <sup>b</sup>	7.39	3.67–14.9	<b>&lt;0.0001*</b>	4.69	2.19–10	<b>0.0001*</b>
IMAC (high) <sup>b</sup>	2.87	1.61–5.12	<b>0.0003*</b>	1.13	0.58–2.19	0.73

CI, confidence interval; HR, hazard ratio; IMAC, intramuscular adipose tissue content; PMI, psoas muscle mass index.

<sup>a</sup>The median age at surgery in this cohort was 68 years.

<sup>b</sup>Cut-off thresholds of PMI/IMAC were determined by receiver operating characteristic analysis with Youden's index for overall survival in colorectal cancer patients.

\***P < 0.05**. Bold font means significant *p*-value in these tables.

**Table 2B** Multivariate analysis for predictors of disease-free survival

Variable	Univariate			Multivariate		
	HR	95% CI	P value	HR	95% CI	P value
Gender (male)	0.79	0.41–1.52	0.49			
Age (>68 years old) <sup>a</sup>	1.02	0.53–1.95	0.95			
Histological type (undifferentiated)	2.76	1.15–6.62	<b>0.023*</b>	1.11	0.42–2.91	0.83
Location (left)	0.81	0.41–1.61	0.55			
T classification (pT3/4)	4.08	1.59–10.5	<b>0.004*</b>	2.22	0.73–6.72	0.16
Vessel involvement (present)	2.6	1.35–4.99	<b>0.004*</b>	1.29	0.59–2.81	0.52
Lymphatic vessel involvement (present)	3.05	1.19–7.84	<b>0.021*</b>	1.09	0.34–3.49	0.88
Lymph node metastasis (present)	3.83	1.99–7.35	<b>0.0001*</b>	2.51	1.23–5.15	<b>0.012*</b>
PMI (low) <sup>b</sup>	3.28	1.7–6.34	<b>0.0004*</b>	2.33	1.14–4.77	<b>0.021*</b>
IMAC (high) <sup>b</sup>	3.16	1.64–6.1	<b>0.0006*</b>	2	0.96–4.2	0.06

CI, confidence interval; HR, hazard ratio; IMAC, intramuscular adipose tissue content; PMI, psoas muscle mass index.

<sup>a</sup>The median age at surgery in this cohort was 68 years.

<sup>b</sup>Cut-off thresholds of PMI/IMAC were determined by receiver operating characteristic analysis with Youden's index for disease-free survival in colorectal cancer patients.

\***P < 0.05**. Bold font means significant *p*-value in these tables.

skeletal muscles mass (decreased PMI) in CRC patients. We thus next examined the potential functional role of miR-203 in myopenia in CRC patients. To investigate the function of miR-203 in human SkMCs, we transfected miR-203 mimic and miRNA negative control mimic into SkMCs and confirmed increased miR-203 levels in the miR-203 mimic-transfected cells (Figure 2A). We first evaluated the impact of miR-203 expression on cell proliferation using MTT assays in transfected cells. Proliferation of SkMCs was moderately suppressed 7 days after miR-203 mimic transfection compared with negative control-transfected cells (Figure 2B). Further, cell cycle analysis revealed that the G<sub>0</sub>/G<sub>1</sub>-phase fraction was slightly increased after miR-203 overexpression (Figure 2C). We next examined whether miR-203 overexpression affects apoptosis in human SkMCs. Because of the highlight of this miR-203 function in SkMCs, we examined cell apoptosis using two methods. Flow cytometry after annexin V and 7-amino-actinomycin D staining demonstrated that SkMCs transfected

with miR-203 mimic showed a significantly increased apoptosis rate compared with negative control-transfected cells (*P* < 0.001, Figure 2D). Furthermore, we also used MTT assay to evaluate the number of viable SkMCs and found a significant decrease of viable cells in SkMCs transfected with miR-203 compared with negative control-transfected cells (*P* < 0.001, Figure 2E).

### Identification of BIRC5 as target of miR-203 in skeletal muscle cells

To elucidate the molecular mechanisms underlying the cellular effects of miR-203 in SkMCs, especially apoptosis, we searched for potential gene targets of miR-203. Candidate targets were first determined using target prediction engines, including miRMap, MicroT4, TargetScan, and RNAhybrid, and the overlapping candidate genes from these four prediction



**Table 3** Multivariate analysis for predictors of myopenia in CRC patients

Variable	Univariate			Multivariate		
	OR	95% CI	P value	OR	95% CI	P value
Gender (female)	2.33	1.27–4.3	<b>0.007*</b>	2.5	1.13–5.53	<b>0.024*</b>
Age (>68 years old) <sup>a</sup>	1.57	0.86–2.85	0.14			
Histological type (undifferentiated)	0.46	0.16–1.29	0.14			
Location (left)	0.62	0.33–1.17	0.14			
T classification (pT3/4)	2.06	1.04–4.05	<b>0.036*</b>	1.07	0.41–2.79	0.89
Vessel involvement (present)	1.93	1.05–3.53	<b>0.034*</b>	0.75	0.3–1.88	0.54
Lymphatic vessel involvement (present)	2.58	1.21–5.5	<b>0.014*</b>	1.97	0.62–6.26	0.25
Lymph node metastasis (present)	2.72	1.47–5.04	<b>0.001*</b>	1.71	0.72–4.07	0.22
Distant metastasis (present)	3.06	1.49–6.31	<b>0.002*</b>	1.42	0.5–4.07	0.51
Pre-operative haemoglobin (low) <sup>b</sup>	4.11	2.18–7.77	<b>&lt;0.0001*</b>	3.1	1.36–7.08	<b>0.007*</b>
Pre-operative lymphocytes (low) <sup>b</sup>	0.55	0.27–1.09	0.09			
Pre-operative albumin (low) <sup>b</sup>	4.69	2.44–9.02	<b>&lt;0.0001*</b>	3.21	1.36–7.58	<b>0.008*</b>
Pre-operative serum miR-203 (high) <sup>b</sup>	5.46	2.32–12.8	<b>0.0001*</b>	5.16	1.8–14.8	<b>0.002*</b>

CI, confidence interval; CRC, colorectal cancer; OR, odds ratio.

<sup>a</sup>The median age at surgery is 68 years in CRC patients.

<sup>b</sup>Cut-off thresholds of each covariate were determined by receiver operating characteristic analysis with Youden's index for myopenia in each gender of CRC patients.

\* $P < 0.05$ . Bold font means significant  $p$ -value in these tables.

engines were selected for analyses. Based on our *in vitro* experiments indicating a role for miR-203 in apoptosis, we focused the apoptosis pathway-associated genes among the overlapping gene pool, especially *CASP3*, *CASP10*, *BIRC5* (survivin), *BMI1*, *BIRC2*, and *BIRC3* (Figure 2F). We examined the expression profiles of these six genes in SkMCs transfected with miR-203 mimic transfection or negative control. Among all six examined genes, only *BIRC5* expression was drastically decreased in miR-203 mimic-transfected cells compared with negative control cells (Figure 2G). Furthermore, fluorescent immunocytochemistry clearly revealed that the protein expression of BIRC5 was also down-regulated in miR-203 mimic-transfected cells (Figure 2H). This result is consistent with a recent study that revealed the regulatory interaction between miR-203 and the 3' untranslated region of BIRC5 mRNA in HEK293T cells using luciferase assays.<sup>40</sup> *BIRC5* (survivin) is a member of the apoptosis inhibitor protein family and could suppress apoptosis via inhibition of the initiator caspase 9 and executioner caspase 3 and 7.<sup>41</sup> In addition, survivin has the potential role as a regulator of cell division especially in G<sub>1</sub>/S arrest of the cell cycle.<sup>42</sup> Taken together, these results successfully validated the clinical finding of a negative correlation between circulating miR-203 expression and pre-operative PMI levels. Our data suggest that elevated expression of circulating miR-203 from metastatic tissues might be involved in myopenia by inducing apoptosis of SkMCs via inhibition of survivin in CRC patients.

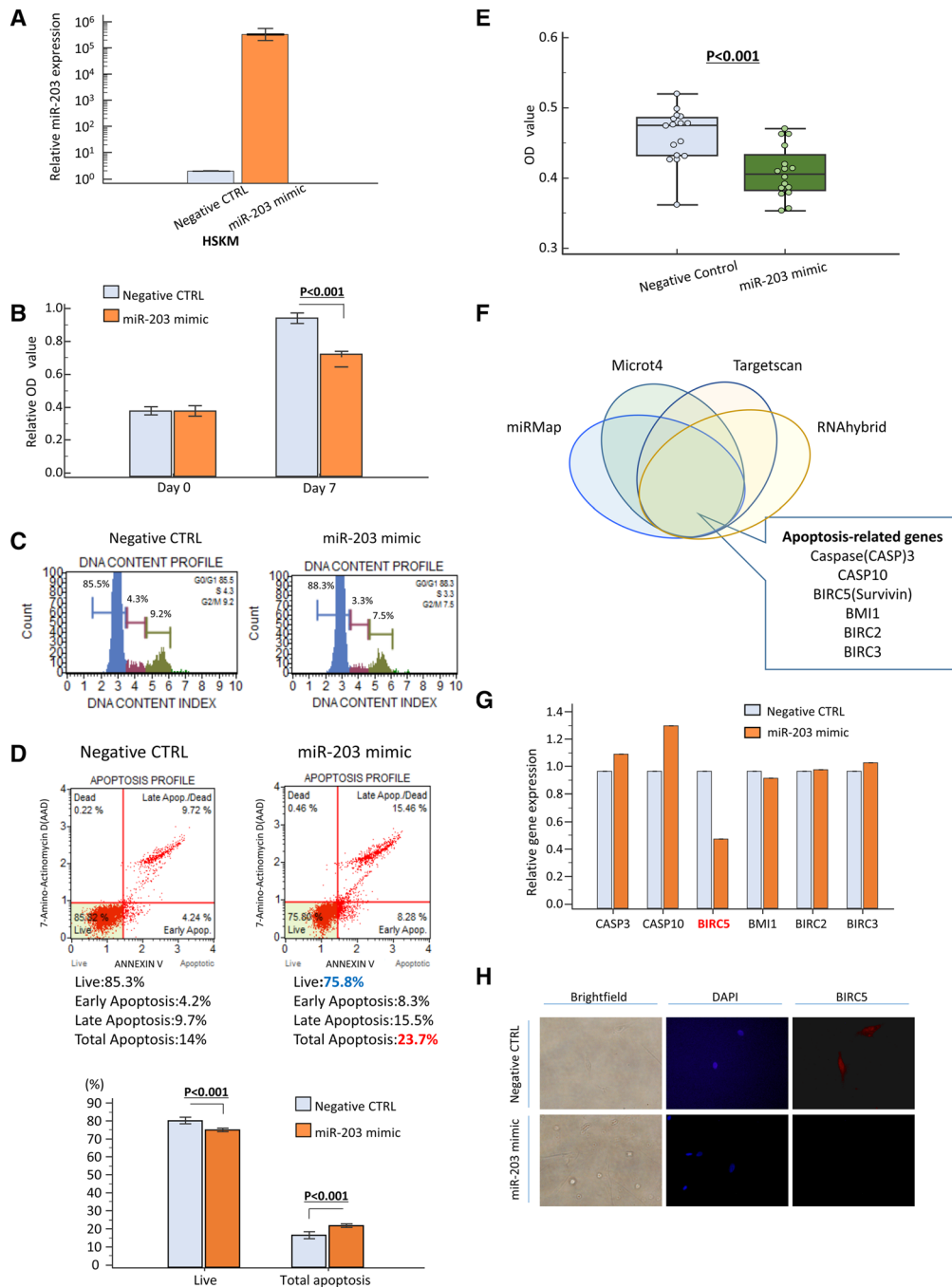
## Discussion

Sarcopenia is a progressive decline of skeletal muscle mass, quality, and strength in response to various factors, including ageing, lifestyle habits, inactivity, and chronic disease.<sup>43</sup>

Although accumulating evidence has demonstrated high prevalence of sarcopenia in cancer patients with metastasis,<sup>10,12,13</sup> the detailed mechanism that drives sarcopenia is not fully understood. We investigated whether alteration of BC could correlate with the circulating metastasis-related miRNA miR-203 in CRC patients, and our study presents several novel findings. First, we systematically investigated pre-operative BC status in CRC patients and demonstrated that both decreased PMI and increased IMAC were significantly correlated with poor prognosis of OS and DFS in CRC patients. In particular, decreased PMI was significantly correlated with all well-established clinicopathological factors for CRC development and was an independent prognostic marker for OS and DFS in CRC patients. Second, miR-203 expressions in primary CRC tissue and matched serum specimens were evaluated, and we found that serum miR-203 expression, but not tissue miR-203 expression, was negatively correlated with pre-operative PMI in CRC patients. Furthermore, multivariate logistic regression analysis revealed that elevated serum miR-203 was an independent risk factor for low PMI (myopenia) in CRC patients. These findings combined with previous evidence from our group<sup>21</sup> suggest that skeletal muscle might be decreased in metastatic CRC patients by circulating miR-203 released from metastatic tissues. We performed a series of *in vitro* analyses and confirmed that miR-203 overexpression significantly promoted apoptosis in human SkMCs, possibly through its down-regulation of survivin.

A high prevalence of sarcopenia in metastatic cancer patients is well documented.<sup>13,26</sup> Although several factors, such as anorexia due to organ dysfunction by distant metastasis, adverse effect of systemic chemotherapy, deterioration of physical activity, and psychological factors for disease development, can induce sarcopenia in patients, emerging evidence has suggested that sarcopenia may develop because of secretory products from metastatic tissues in various

**Figure 2** Series of *in vitro* analysis using human skeletal muscle cells (SkMCs). (A) Overexpression of miR-203 expression 48 h after transfection in SkMC line. (B) Effect of miR-203 overexpression on SkMC proliferation as assessed by MTT assay. (C) Cell cycle analysis demonstrated that G<sub>0</sub>/G<sub>1</sub> fraction was increased after miR-203 overexpression. (D, E) Apoptosis assay to investigate the population of apoptotic cells and viable cells of SkMCs after miR-203 overexpression. Apoptosis rates were measured by annexin V and 7-amino-actinomycin D (7-AAD) staining, and apoptotic cells were calculated as upper right and lower right (D): negative control (CTRL): right panel; miR-203 mimic: left panel. Rate of apoptotic cells was significantly increased after miR-203 overexpression ( $P < 0.05$ , lower panel). The number of viable cancer cells was also calculated by MTT assay and showed that miR-203 up-regulation decreased the number of viable SkMCs (E). (F) Prediction of miR-203 target gene via four different miRNA target prediction tools (miRMap, Microt4, Targetscan, and RNAhybrid). (G) Expression profile of apoptosis-related genes about putative targets of miR-203 showed that overexpression of miR-203 suppressed BIRC5 expression in SkMCs. Expression profile of apoptosis-related genes about putative targets of miR-203 showed that overexpression of miR-203 suppressed BIRC5 expression in SkMCs. (H) BIRC5 protein was expressed in both nucleus and cytoplasm in SkMCs and was down-regulated in miR-203 mimic-transfected cells compared with negative CTRL cells. Each value represents the mean  $\pm$  standard error. OD, optical density.



malignancies.<sup>10,44</sup> Waning and co-workers established seven different mouse models of human osteolytic bone metastases and reported impaired muscle dysfunction in these mice. The authors performed unbiased mass spectrometry-based screening to assess the post-transcriptional modification of proteins in whole skeletal muscle lysates from mice with or without bone metastasis and found that transforming growth factor (TGF)- $\beta$ , released from the bone surface during metastasis-induced bone destruction, could induce oxidization of skeletal muscle proteins, impair intracellular signalling in SkMCs, and decrease muscle contraction.<sup>10</sup> In line with this evidence, a recent study revealed metal-ion transporter XRT-like and IRT-like protein 14 (ZIP14) as a critical mediator of metastatic cancer-induced cachexia.<sup>44</sup> The authors performed allografts using a metastatic subline of mouse breast and colon cancer cell lines, and sequencing-based comprehensive analysis using cachexic tibialis anterior muscles showed that ZIP14 was significantly up-regulated in the cachexic muscles from metastatic models. ZIP14 expression was induced in SkMCs by TGF- $\alpha$  and TGF- $\beta$  cytokines, and ZIP14-mediated zinc uptake resulted in blocking muscle cell differentiation and myosin heavy chain loss.<sup>44</sup> Collectively, these results suggested that metastasis-induced sarcopenia may develop from the interaction between the systemic circulation and the local micro-environment of skeletal muscle in patients with malignancies.

In contrast, as a role for miRNAs in myogenesis has been established,<sup>45</sup> the pivotal function of miRNAs in sarcopenia development is also being elucidated. Connolly and colleagues conducted screening of miRNA expression using quadriceps specimens from chronic obstructive lung disease patients with or without muscle wasting and revealed that elevated miR-542-3p/5p induces muscle atrophy through the promotion of mitochondrial dysfunction and activation of SMAD2/3 phosphorylation.<sup>46</sup> This research group then recently showed that increased expression of miR-424-5p in quadriceps is also significantly correlated with sarcopenia via regulation of ribosomal RNA synthesis.<sup>47</sup> Furthermore, in researching the function of circulating miRNAs in the pathogenesis of cancer sarcopenia, He and colleagues demonstrated that elevated expression of miR-21 in tumour-secreted macrovesicles promotes myoblast apoptosis in cancer cachexia via a toll-like receptor 7-c-Jun N-terminal kinase-dependent pathway.<sup>48</sup>

Combined with these data, we hypothesized that circulating miRNAs released from metastatic tissues might have the potential to induce sarcopenia in advanced cancer patients with distant metastasis. In this study, we performed a direct comparison between pre-operative BC status and tissue or serum miR-203 expression in CRC patients and revealed an inverse correlation between PMI levels and serum miR-203 expression. Furthermore, elevated serum miR-203 levels were an independent risk factor for low PMI (myopenia) in CRC patients. We validated our clinical findings using a series

of *in vitro* analyses and demonstrated that miR-203 can induce apoptosis via down-regulation of survivin in human SkMCs. These findings help further the current research field of pathogenesis in metastasis-related sarcopenia in malignancies.

Sarcopenia is generally defined as a syndrome characterized by progressive and generalized loss of skeletal muscle mass and strength, and the European Working Group on Sarcopenia recommended that the definition of sarcopenia should include both low muscle mass and low muscular function.<sup>49</sup> Based on these recommendations, the pattern of sarcopenia is currently divided into 'myopenia' and 'myosteatorsis'. Myopenia is characterized by decreased skeletal muscle mass irrespective of illness and ageing, and PMI is recognized as one of representative surrogate markers for assessment of skeletal muscle mass.<sup>6,50</sup> In contrast, myosteatorsis, which is usually assessed by IMAC, is characterized by an increased infiltration of intermuscular and intramuscular fat.<sup>51</sup> One of the novel findings in our study is the intimate correlation between disease development factors and myopenia despite the lack of those correlation with myosteatorsis in CRC patients. Furthermore, our previous study clearly demonstrated that miR-203 could be secreted from various metastatic tissues including lymph node, peritoneal, and hepatic metastasis, in CRC patients.<sup>21</sup> In contrast, several studies indicated that intermuscular and intramuscular fatty accumulation arise through several different pathways, including insulin resistance, inflammation, adipogenesis, inhibition of histone deacetylases, and oestrogen deficiency, and suggested that these various conditions might induce myosteatorsis.<sup>52</sup> Collectively, these evidences with our novel finding regarding the apoptotic role of over-expressed miR-203 in SkMCs could explain the reason why circulating miR-203 levels significantly correlated with myopenia, not myosteatorsis in CRC patients.

We acknowledge several potential limitations of the present study. First, we only focused on metastatic tissues secreting miR-203 in this study. Further studies including a broader, unbiased comprehensive analysis based on our concept could potentially lead to the identification of additional secretory miRNAs to promote myopenia and cachexia in patients with various malignancies. Furthermore, unfortunately, we could not assess the post-operative serum specimens from these patients and evaluate the potential of circulating miR-203 to monitor the status of myopenia in CRC patients. Therefore, further studies including long-term follow-up of BC, along with monitoring of serum miRNA, may be needed to confirm the clinical feasibility of serum miR-203 for real-time monitoring of myopenia during peri-operative period. Together, our results suggest that quantification of serum miR-203 expression could be used as a risk assessment of myopenia in CRC patients and that miR-203 might be a novel therapeutic target for inhibition of myopenia in CRC.

## Acknowledgements

The authors thank Yuki Orito and Amphone Okada for their excellent technical assistance. We thank Edanz Group ([www.edanzediting.com/ac](http://www.edanzediting.com/ac)) for editing a draft of this manuscript. The authors certify that they comply with the ethical guidelines for publishing in the *Journal of Cachexia, Sarcopenia and Muscle: update 2017*.<sup>53</sup>

## Conflict of interest

None declared.

## Funding

This work was supported by R01 (CA72851, CA18172, and CA184792) and U01 (CA187956) grants from the National Cancer Institute, NIH and grants from the Baylor Foundation and Baylor Scott & White Research Institute, Dallas, TX, USA, to A. G. In addition, this study was also supported by the research grant from the Japanese Society for Palliative Medicine and the Japanese Society for Parenteral and Enteral Nutrition to Y.O.

## References

1. Fearon K, Strasser F, Anker SD, Bosaeus I, Bruera E, Fainsinger RL, et al. Definition and classification of cancer cachexia: an international consensus. *Lancet Oncol* 2011;**12**:489–495.
2. Cohen S, Nathan JA, Goldberg AL. Muscle wasting in disease: molecular mechanisms and promising therapies. *Nat Rev Drug Discov* 2015;**14**:58–74.
3. Sandri M. Protein breakdown in cancer cachexia. *Semin Cell Dev Biol* 2016;**54**:11–19.
4. Argiles JM, Busquets S, Stemmler B, Lopez-Soriano FJ. Cancer cachexia: understanding the molecular basis. *Nat Rev Cancer* 2014;**14**:754–762.
5. Muscaritoli M, Anker SD, Argiles J, Aversa Z, Bauer JM, Biolo G, et al. Consensus definition of sarcopenia, cachexia and pre-cachexia: joint document elaborated by Special Interest Groups (SIG) “cachexia-anorexia in chronic wasting diseases” and “nutrition in geriatrics”. *Clinical nutrition (Edinburgh, Scotland)* 2010;**29**:154–159.
6. Okumura S, Kaido T, Hamaguchi Y, Fujimoto Y, Masui T, Mizumoto M, et al. Impact of preoperative quality as well as quantity of skeletal muscle on survival after resection of pancreatic cancer. *Surgery* 2015;**157**:1088–1098.
7. Kobayashi A, Kaido T, Hamaguchi Y, Okumura S, Taura K, Hatano E, et al. Impact of postoperative changes in sarcopenic factors on outcomes after hepatectomy for hepatocellular carcinoma. *J Hepatobiliary Pancreat Sci* 2016;**23**:57–64.
8. Hamaguchi Y, Kaido T, Okumura S, Kobayashi A, Hamad A, Tamai Y, et al. Proposal for new diagnostic criteria for low skeletal muscle mass based on computed tomography imaging in Asian adults. *Nutrition* 2016;**32**:1200–1205.
9. Chiang AC, Massague J. Molecular basis of metastasis. *N Engl J Med* 2008;**359**:2814–2823.
10. Waning DL, Mohammad KS, Reiken S, Xie W, Andersson DC, John S, et al. Excess TGF- $\beta$  mediates muscle weakness associated with bone metastases in mice. *Nat Med* 2015;**21**:1262–1271.
11. Penna F, Busquets S, Argiles JM. Experimental cancer cachexia: evolving strategies for getting closer to the human scenario. *Semin Cell Dev Biol* 2016;**54**:20–27.
12. Shiono M, Huang K, Downey RJ, Consul N, Villanueva N, Beck K, et al. An analysis of the relationship between metastases and cachexia in lung cancer patients. *Cancer Med* 2016;**5**:2641–2648.
13. Okugawa Y, Toiyama Y, Yamamoto A, Shigemori T, Yin C, Narumi A, et al. Clinical impact of muscle quantity and quality in colorectal cancer patients: a propensity score matching analysis. *JPEN Journal of parenteral and enteral nutrition*. 2018.
14. Becker A, Thakur BK, Weiss JM, Kim HS, Peinado H, Lyden D. Extracellular vesicles in cancer: cell-to-cell mediators of metastasis. *Cancer Cell* 2016;**30**:836–848.
15. McAllister SS, Weinberg RA. The tumour-induced systemic environment as a critical regulator of cancer progression and metastasis. *Nat Cell Biol* 2014;**16**:717–727.
16. Okugawa Y, Grady WM, Goel A. Epigenetic alterations in colorectal cancer: emerging biomarkers. *Gastroenterology* 2015;**149**(5):1204–25.e12.
17. Okugawa Y, Toiyama Y, Goel A. An update on microRNAs as colorectal cancer biomarkers: where are we and what's next? *Expert Rev Mol Diagn* 2014;**14**:999–1021.
18. Toiyama Y, Okugawa Y, Fleshman J, Richard Boland C, Goel A. MicroRNAs as potential liquid biopsy biomarkers in colorectal cancer: a systematic review. *Biochim Biophys Acta* 2018.
19. Valadi H, Ekstrom K, Bossios A, Sjostrand M, Lee JJ, Lotvall JO. Exosome-mediated transfer of mRNAs and microRNAs is a novel mechanism of genetic exchange between cells. *Nat Cell Biol* 2007;**9**:654–659.
20. Montecalvo A, Larregina AT, Shufesky WJ, Stolz DB, Sullivan ML, Karlsson JM, et al. Mechanism of transfer of functional

## Online supplementary material

Additional supporting information may be found online in the Supporting Information section at the end of the article.

**Table S1.** Primers used for quantitative real time PCR analysis.

**Table S2.** Correlation between body composition and sex in colorectal cancer patients

**Figure S1.** Prognostic impact of body composition status in CRC patients subdivided by sex. (a-d) High IMAC status was significantly correlated with poor OS (a: Male:  $P=0.001$ , c: Female:  $P=0.04$ ) and DFS (b: Male:  $P=0.009$ , d: Female:  $P=0.015$ ) both in male and female patients. (e-h) Decreased PMI significantly correlated with poor prognosis for OS (e: Male:  $P<0.0001$ , g: Female:  $P=0.0002$ ) and DFS (f: Male:  $P=0.004$ , h: Female:  $P=0.026$ ). All statistical tests were log-rank test and two-sided.

**Figure S2.** Correlation between PMI status and various representative nutrition markers in CRC patients. Although number of peripheral lymphocytes did not correlate with PMI status, preoperative hemoglobin and albumin levels were significantly decreased in CRC patients with low PMI (a: hemoglobin, b: albumin, c: lymphocytes). Statistically significant differences were determined using the Mann-Whitney U test.

- microRNAs between mouse dendritic cells via exosomes. *Blood* 2012;**119**:756–766.
21. Hur K, Toiyama Y, Okugawa Y, Ide S, Imaoka H, Boland CR, et al. Circulating microRNA-203 predicts prognosis and metastasis in human colorectal cancer. *Gut* 2017;**66**:654–665.
  22. Luo W, Wu H, Ye Y, Li Z, Hao S, Kong L, et al. The transient expression of miR-203 and its inhibiting effects on skeletal muscle cell proliferation and differentiation. *Cell Death Dis* 2014;**5**:e1347.
  23. Yi R, Poy MN, Stoffel M, Fuchs E. A skin microRNA promotes differentiation by repressing 'stemness'. *Nature* 2008;**452**:225–229.
  24. Edge SB BD CC FA. In Greene FL, Trotti A, eds. *AJCC Cancer Staging Manual*, 7th ed; 2010.
  25. Fujikawa H, Araki T, Okita Y, Kondo S, Kawamura M, Hiro J, et al. Impact of sarcopenia on surgical site infection after restorative proctocolectomy for ulcerative colitis. *Surg Today* 2017;**47**:92–98.
  26. Okugawa Y, Yao L, Toiyama Y, Yamamoto A, Shigemori T, Yin C, et al. Prognostic impact of sarcopenia and its correlation with circulating miR-21 in colorectal cancer patients. *Oncol Rep* 2018;**39**:1555–1564.
  27. Kitajima Y, Eguchi Y, Ishibashi E, Nakashita S, Aoki S, Toda S, et al. Age-related fat deposition in multifidus muscle could be a marker for nonalcoholic fatty liver disease. *J Gastroenterol* 2010;**45**:218–224.
  28. Kitajima Y, Hyogo H, Sumida Y, Eguchi Y, Ono N, Kuwashiro T, et al. Severity of non-alcoholic steatohepatitis is associated with substitution of adipose tissue in skeletal muscle. *J Gastroenterol Hepatol* 2013;**28**:1507–1514.
  29. Kroh EM, Parkin RK, Mitchell PS, Tewari M. Analysis of circulating microRNA biomarkers in plasma and serum using quantitative reverse transcription-PCR (qRT-PCR). *Methods* 2010;**50**:298–301.
  30. Toiyama Y, Takahashi M, Hur K, Nagasaka T, Tanaka K, Inoue Y, et al. Serum miR-21 as a diagnostic and prognostic biomarker in colorectal cancer. *J Natl Cancer Inst* 2013;**105**:849–859.
  31. Hur K, Toiyama Y, Takahashi M, Balaguer F, Nagasaka T, Koike J, et al. MicroRNA-200c modulates epithelial-to-mesenchymal transition (EMT) in human colorectal cancer metastasis. *Gut* 2013;**62**:1315–1326.
  32. Link A, Balaguer F, Shen Y, Nagasaka T, Lozano JJ, Boland CR, et al. Fecal microRNAs as novel biomarkers for colon cancer screening. *Cancer Epidemiol Biomarkers Prev* 2010;**19**:1766–1774.
  33. Chang KH, Mestdagh P, Vandesompele J, Kerin MJ, Miller N. MicroRNA expression profiling to identify and validate reference genes for relative quantification in colorectal cancer. *BMC Cancer* 2010;**10**:173.
  34. Hur K, Toiyama Y, Schetter AJ, Okugawa Y, Harris CC, Boland CR, et al. Identification of a metastasis-specific microRNA signature in human colorectal cancer. *J Natl Cancer Inst* 2015;**107**.
  35. Okugawa Y, Toiyama Y, Toden S, Mitoma H, Nagasaka T, Tanaka K, et al. Clinical significance of SNORA42 as an oncogene and a prognostic biomarker in colorectal cancer. *Gut* 2017;**66**:107–117.
  36. Okugawa Y, Tanaka K, Inoue Y, Kawamura M, Kawamoto A, Hiro J, et al. Brain-derived neurotrophic factor/tropomyosin-related kinase B pathway in gastric cancer. *Br J Cancer* 2013;**108**:121–130.
  37. Okugawa Y, Toiyama Y, Ichikawa T, Kawamura M, Yasuda H, Fujikawa H, et al. Colony-stimulating factor-1 and colony-stimulating factor-1 receptor co-expression is associated with disease progression in gastric cancer. *Int J Oncol* 2018;**53**:737–749.
  38. Delitto D, Judge SM, George TJ Jr, Sarosi GA, Thomas RM, Behrns KE, et al. A clinically applicable muscular index predicts long-term survival in resectable pancreatic cancer. *Surgery* 2017;**161**:930–938.
  39. Okugawa Y, Toiyama Y, Yamamoto A, Shigemori T, Kitamura A, Ichikawa T, et al. Close relationship between immunological/inflammatory markers and myopenia and myosteatosis in patients with colorectal cancer: a propensity score matching analysis. *JPEN Journal of parenteral and enteral nutrition* 2018.
  40. Zhang X, Zhang Y, Liu X, Fang A, Li P, Li Z, et al. MicroRNA-203 is a prognostic indicator in bladder cancer and enhances chemosensitivity to cisplatin via apoptosis by targeting Bcl-w and survivin. *PLoS one* 2015;**10**:e0143441.
  41. Kotipatruni RR, Nalla AK, Asuthkar S, Gondi CS, Dinh DH, Rao JS. Apoptosis induced by knockdown of uPAR and MMP-9 is mediated by inactivation of EGFR/STAT3 signaling in medulloblastoma. *PLoS one*. 2012;**7**:e44798.
  42. Dai D, Liang Y, Xie Z, Fu J, Zhang Y, Zhang Z. Survivin deficiency induces apoptosis and cell cycle arrest in HepG2 hepatocellular carcinoma cells. *Oncol Rep* 2012;**27**:621–627.
  43. Baumgartner RN, Koehler KM, Gallagher D, Romero L, Heymsfield SB, Ross RR, et al. Epidemiology of sarcopenia among the elderly in New Mexico. *Am J Epidemiol* 1998;**147**:755–763.
  44. Wang G, Biswas AK, Ma W, Kandpal M, Coker C, Grandgenett PM, et al. Metastatic cancers promote cachexia through ZIP14 upregulation in skeletal muscle. *Nat Med* 2018;**24**:770–781.
  45. Horak M, Novak J, Bienertova-Vasku J. Muscle-specific microRNAs in skeletal muscle development. *Dev Biol* 2016;**410**:1–13.
  46. Garros RF, Paul R, Connolly M, Lewis A, Garfield BE, Natanek SA, et al. MicroRNA-542 promotes mitochondrial dysfunction and SMAD activity and is elevated in intensive care unit-acquired weakness. *Am J Respir Crit Care Med* 2017;**196**:1422–1433.
  47. Connolly M, Paul R, Farre-Garros R, Natanek SA, Bloch S, Lee J, et al. miR-424-5p reduces ribosomal RNA and protein synthesis in muscle wasting. *J Cachexia Sarcopenia Muscle* 2018;**9**:400–416.
  48. He WA, Calore F, Londhe P, Canella A, Guttridge DC, Croce CM. Microvesicles containing miRNAs promote muscle cell death in cancer cachexia via TLR7. *Proc Natl Acad Sci U S A* 2014;**111**:4525–4529.
  49. Cruz-Jentoft AJ, Baeyens JP, Bauer JM, Boirie Y, Cederholm T, Landi F, et al. Sarcopenia: European consensus on definition and diagnosis: report of the European Working Group on Sarcopenia in Older People. *Age Ageing* 2010;**39**:412–423.
  50. Fearon K, Evans WJ, Anker SD. Myopenia—a new universal term for muscle wasting. *J Cachexia Sarcopenia Muscle* 2011;**2**:1–3.
  51. Miljkovic I, Zmuda JM. Epidemiology of myosteatosis. *Curr Opin Clin Nutr Metab Care* 2010;**13**:260–264.
  52. Hamrick MW, McGee-Lawrence ME, Frechette DM. Fatty infiltration of skeletal muscle: mechanisms and comparisons with bone marrow adiposity. *Front Endocrinol* 2016;**7**:69.
  53. von Haehling S, Morley JE, Coats AJS, Anker SD. Ethical guidelines for publishing in the journal of cachexia, sarcopenia and muscle: update 2017. *J Cachexia Sarcopenia Muscle* 2017;**8**:1081–1083.